

LETTER

Scaling metabolism from individuals to reef-fish communities at broad spatial scales

D. R. Barneche,¹ M. Kulbicki,^{2,3}
S. R. Floeter,⁴ A. M. Friedlander,⁵
J. Maina⁶ and A. P. Allen¹

Abstract

Fishes contribute substantially to energy and nutrient fluxes in reef ecosystems, but quantifying these roles is challenging. Here, we do so by synthesising a large compilation of fish metabolic-rate data with a comprehensive database on reef-fish community abundance and biomass. Individual-level analyses support predictions of Metabolic Theory after accounting for significant family-level variation, and indicate that some tropical reef fishes may already be experiencing thermal regimes at or near their temperature optima. Community-level analyses indicate that total estimated respiratory fluxes of reef-fish communities increase on average ~2-fold from 22 to 28 °C. Comparisons of estimated fluxes among trophic groups highlight striking differences in resource use by communities in different regions, perhaps partly reflecting distinct evolutionary histories, and support the hypothesis that piscivores receive substantial energy subsidies from outside reefs. Our study demonstrates one approach to synthesising individual- and community-level data to establish broad-scale trends in contributions of biota to ecosystem dynamics.

Keywords

Allometry, climate change, ecosystem function, coral reef, metabolic theory of ecology, food web, acclimation.

Ecology Letters (2014) **17**: 1067–1076

INTRODUCTION

Reef fishes are a diverse group of vertebrates, comprising > 6000 species (Parravicini *et al.* 2013). They play key roles in the flow of energy and nutrients through many reef ecosystems (Polovina 1984; Arias-González *et al.* 1997; Bozec *et al.* 2004), but quantifying these roles, and how they may be affected by future climate change, remains an important research challenge (Wilson *et al.* 2010). An essential step in meeting this challenge entails characterising the trophic structures and energy fluxes of reef-fish communities, and how they vary with broad-scale gradients in key variables such as temperature and productivity.

Metabolic rate is a fundamental determinant of an organism's contribution to energy and nutrient flux in an ecosystem (Brown *et al.* 2004; Allen *et al.* 2005). The metabolic rate per unit body mass (i.e. mass-specific rate) generally declines with body mass, but increases with temperature (Gillooly *et al.* 2001; Brown *et al.* 2004). Consequently, given that the energy flux of a community is equal to the sum of the individual metabolic rates (Allen *et al.* 2005), changes in temperature, size structure and/or standing biomass of a given community may affect its energetics and

resource use, and hence its contribution to ecosystem structure and function (Sandin *et al.* 2008; Mora *et al.* 2011; McDole *et al.* 2012). Conversely, communities that are distinct with respect to these variables may be energetically similar (Fig. 1). The Metabolic Theory of Ecology (MTE; Brown *et al.* 2004) yields predictions for how community abundance, biomass and energy flux should change with size structure, temperature and ecosystem productivity (Allen *et al.* 2005; Yvon-Durocher & Allen 2012; Trebilco *et al.* 2013), but there have been few attempts to test such predictions (but see Lopez-Urrutia *et al.* 2006; O'Connor *et al.* 2009; McDole *et al.* 2012), particularly at broad spatial scales.

Here, we use MTE as a framework to synthesise individual- and community-level data and analyses (Fig. 1) to estimate energy fluxes and trophic structures of reef-fish communities and how they change along gradients of temperature and productivity. Our approach builds on other recent studies that use MTE to quantify the energetics of marine communities and ecosystems (Lopez-Urrutia *et al.* 2006; O'Connor *et al.* 2009; McDole *et al.* 2012), and a much larger body of earlier work that yielded predictions on ecosystem dynamics by summing metabolic rates of individu-

¹Department of Biological Sciences, Macquarie University, 2109, Sydney, NSW, Australia

²IRD (Institut de Recherche pour le Développement), UR-CoRéUs, Laboratoire Arago, BP 44, 66651, Banyuls/mer, France

³CESAB-FRB, Immeuble Henri Poincaré, Domaine du Petit Arbois, 13857, Aix-en-Provence Cedex 3, France

⁴Departamento de Ecologia e Zoologia, Universidade Federal de Santa Catarina, 88010-970, Florianópolis, Santa Catarina, Brazil

⁵Fisheries Ecology Research Lab, Department of Biology, University of Hawaii, 96822, Honolulu, Hawaii, USA

⁶ARC Centre of Excellence for Environmental Decisions (CEED), The University of Queensland, 4072, Brisbane, Qld, Australia

*Correspondence: E-mail: barnechedr@gmail.com

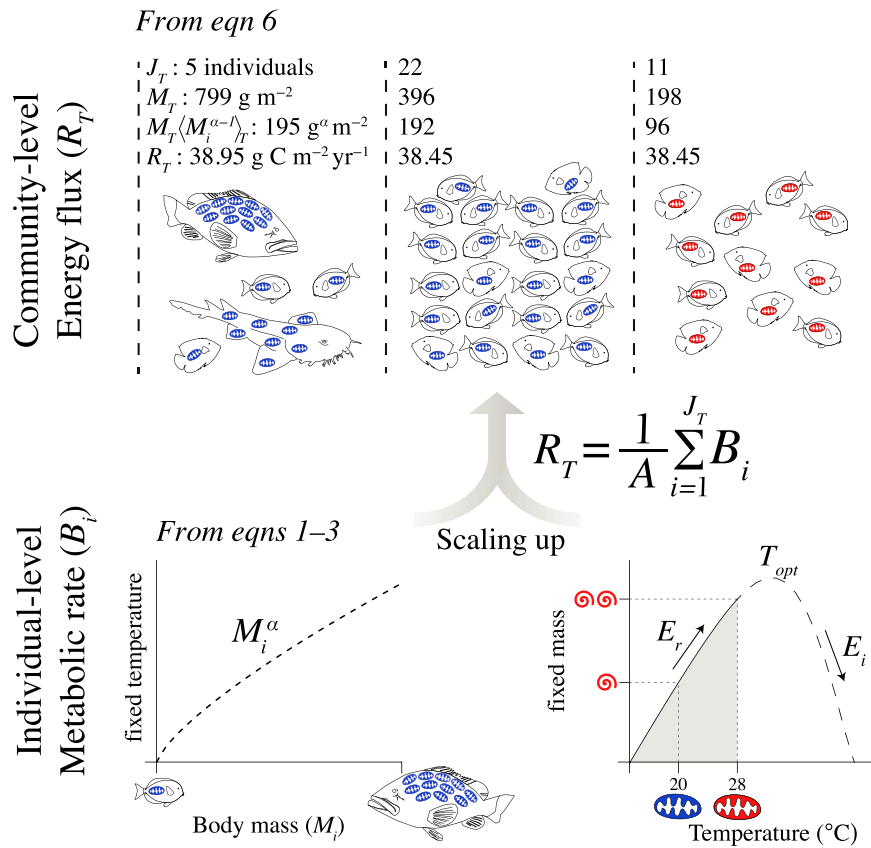


Figure 1 Scaling from individual-level metabolic rate (B_i) to total community-level respiration (R_T). Individual-level rates (lower graphs) exhibit sub-linear power-function scaling with body mass (M_i), implying that the scaling exponent α is < 1 and that respiratory capacity (depicted as mitochondria) per unit body mass declines as size increases. Effects of temperature on rates are exponential well below the optimum. In the hypothetical example, ATP turnover per mitochondrion (spirals) doubles from 20 °C (blue) to 28 °C (red). Community-level flux (in 1 m² area, upper graphs) is similar despite the fact that communities differ in number of individuals (J_T), standing biomass (M_T), size-corrected biomass ($M_T \langle M_i^{\alpha-1} \rangle_T$) and temperature. From left to right, the first and second communities differ in size structure, but are very similar in $M_T \langle M_i^{\alpha-1} \rangle_T$ and environmental temperature (20 °C), and therefore equivalent in terms of respiration. The third community has low M_T , but is found at 28 °C, and therefore respire similarly. Equations 1–6 are detailed in Methods.

als (e.g. Polovina 1984). The community-level database we use encompasses 49 reef sites in eight regions, 496 748 individuals and 989 species. While a number of studies have assessed spatial gradients in biomass and abundance for reef fishes (e.g. Mora *et al.* 2011), to our knowledge, no studies have attempted to quantify energy fluxes of reef-fish communities at such broad spatial scales.

Our analysis entails two distinct components. First, we quantify metabolic rates of fish and their primary determinants and, in so doing, test three predictions of MTE (hypotheses H1–H3 detailed in Methods). Second, we scale up the individual-level scaling relationships to first estimate energy fluxes of communities (e.g. Allen *et al.* 2005; Yvon-Durocher *et al.* 2012) (Fig. 1), and then derive and test predictions on how community-level energy flux should vary with temperature and net primary productivity (NPP) if specific community- and ecosystem-level assumptions are upheld (hypotheses H4–H5). For this second component, we synthesise individual- and community-level data and analyses using a Bayesian approach, building on recent work (Yvon-Durocher & Allen 2012).

METHODS

Individual-level hypotheses

Hypothesis H1: Metabolic rate will increase sub-linearly with body mass according to a power function with a scaling exponent $\alpha \approx 0.75$.

The single best predictor of metabolism across the diversity of life is body mass (Gillooly *et al.* 2001; Brown *et al.* 2004), which varies by > 6 orders of magnitude among reef fishes (Froese & Pauly 2012). The effect of individual body mass, M_i (g), on metabolic rate, B_i (g C d⁻¹), can be characterised by a power function of the form

$$B_i = B_o M_i^\alpha, \quad (1)$$

where B_o is a metabolic normalisation (g C g ^{$-\alpha$} d⁻¹) that varies among taxa and with other variables (Brown *et al.* 2004). The dimensionless scaling exponent α is generally < 1 for metazoans, indicating sub-linear scaling with body mass, and also varies among metazoan taxa, with an average of ~ 0.75

(Savage *et al.* 2004). Previous analyses suggest that *basal* metabolic rates of fish may exhibit a somewhat steeper size scaling (i.e. $\alpha \approx 0.80$; Clarke & Johnston 1999). Here, we assess the scaling of *routine* metabolic rate, which corresponds to the rate of energy expenditure required by a fish in the field to sustain survival, growth and reproduction.

Hypothesis H2: Metabolic-rate temperature dependence can be approximated by the Boltzmann relationship with an activation energy $E_r \approx 0.6$ – 0.7 eV at temperatures below the optimum, T_{opt} .

Another key determinant of metabolic rate is temperature. In general, metabolic rate exhibits a unimodal response (Huey & Stevenson 1979) such that the effects of temperature are positive and exponential at temperatures well below the temperature optimum owing to biochemical kinetics (Gillooly *et al.* 2001), but negative above this optimum owing to protein denaturation and/or other processes that compromise biological function (bottom right plot of Fig. 1). Here, we model these effects of temperature on the metabolic normalisation, B_o from eqn 1, using the following expression (see Supplementary Information),

$$B_o = b_o(T_c) e^{E_r \left(\frac{1}{kT_c} - \frac{1}{kT} \right)} I(T) \quad (2)$$

$$I(T) = \left(1 + \left(\frac{E_r}{E_i - E_r} \right) e^{E_i \left(\frac{1}{kT_{opt}} - \frac{1}{kT} \right)} \right)^{-1}, \quad (3)$$

where $b_o(T_c)$ is the value of the metabolic normalisation at some arbitrary absolute temperature T_c (K), and k is Boltzmann's constant (8.62×10^{-5} eV K $^{-1}$). In this expression, the Boltzmann relationship, $e^{E_r \left(\frac{1}{kT_c} - \frac{1}{kT} \right)}$, describes temperature-induced enhancement of rates using an activation energy, E_r (eV), consistent with previous MTE work (Gillooly *et al.* 2001; Allen *et al.* 2005), whereas $I(T)$ characterises declines in rates above T_{opt} using an inactivation parameter E_i (Schoolfield *et al.* 1981). The existence of a temperature optimum implies that $E_i > E_r$. Previous work indicates that E_r varies among taxonomic groups, with an average of ~ 0.65 eV, which corresponds closely to the average activation energy of metabolic reactions in the respiratory complex (Gillooly *et al.* 2001). In the absence of temperature inactivation, this value for E_r would imply a ~ 3.3 -fold increase in individual energy flux over the range of temperatures experienced by reef fishes (~ 18 – 32 °C). However, if the upper bound of this range is at or near the temperature optimum for reef-fish species, as suggested by some recent work (Gardiner *et al.* 2010), the overall temperature response will be weaker. We can evaluate this hypothesis by statistically comparing models fitted with and without the inactivation term, $I(T)$, in eqns 2 and 3.

Hypothesis H3: The size- and temperature-corrected rate of metabolism, $b_o(T_c)$, is independent of average thermal regime.

While the exponential effects of temperature on biochemical reaction rates have long been recognised, organisms utilise diverse physiological mechanisms to maintain homeostasis in different thermal regimes (Hochachka & Somero 2002). Consequently, some have argued that physiological acclima-

tion and/or evolutionary adaptation may allow organisms that occupy distinct thermal regimes to modulate acute temperature effects, as expressed in eqns 2 and 3, through changes in $b_o(T_c)$ (Clarke & Fraser 2004). We can evaluate this hypothesis by fitting a function of the form

$$b_o(T_c) = \overline{b_o(T_c)} e^{E_a \left(\frac{1}{kT} - \frac{1}{kT_c} \right)}, \quad (4)$$

where $\overline{b_o(T_c)}$ is the size- and temperature-corrected metabolic rate of an organism whose average thermal regime is $\langle 1/kT \rangle$, and E_a characterises any changes in this rate with average thermal regime, $\langle 1/kT \rangle$. We refer to E_a as an adaptation parameter (rather than an activation energy) because it cannot be justified based on simple biochemical kinetics. Nevertheless, it provides a useful benchmark for comparison with the activation energy, E_r , in eqns 2 and 3 above. The evolutionary adaptation hypothesis, as articulated by Clarke & Fraser (2004), proposes that $b_o(T_c)$ is generally higher for taxa adapted to cooler environments, implying that $E_a > 0$ in eqn 4. By contrast, if $E_a \approx 0$, $b_o(T_c)$ is essentially independent of thermal regime, as assumed in the original MTE formulation (Gillooly *et al.* 2001), meaning that temperature scaling of rates is similar within and among taxa. Distinguishing between these alternative hypotheses is particularly relevant here because the existence of temperature adaptation ($E_a > 0$) would imply that the overall temperature-induced enhancement of rates for communities that occupy warmer environments is weaker than would be predicted based solely on the activation energy E_r .

Testing hypotheses H1–H3

The predicted effects of body size ($\alpha \approx 0.75$), temperature ($E_r \approx 0.6$ – 0.7 eV) and thermal regime ($E_a \approx 0$ eV) can be evaluated by combining eqns 1–4 and then taking logarithms to yield

$$\ln B_i = \ln \overline{b_o(T_c)} + \alpha \ln M_i + E_a \left(\left\langle \frac{1}{kT} \right\rangle - \frac{1}{kT_c} \right) + E_r \left(\frac{1}{kT_c} - \frac{1}{kT} \right) - \ln \left(1 + \left(\frac{E_r}{E_i - E_r} \right) e^{E_i \left(\frac{1}{kT_{opt}} - \frac{1}{kT} \right)} \right). \quad (5)$$

We evaluate these predictions using metabolic-rate data compiled in FishBase (Froese & Pauly 2012), along with additional reef-fish data compiled from the recent literature (Supplementary Information). The FishBase data we analyse include all measurements of routine metabolic rate that have accompanying size and temperature data, except measurements denoted as being taken under stressful conditions. To allow for the assessment of differences among families in the temperature scaling of rates (described below), we only include data from families with at least five metabolic-rate measurements over at least a 5 °C temperature range. Data for two families (Carangidae and Coryphaenidae) were, however, excluded because preliminary analyses indicated that they were outliers with respect to scaling behaviour, and therefore prevented statistical models (described below) from converging on stable parameters estimates. In total, our compilation of metabolic-rate data encompasses 2036 measurements taken from 43

families and 270 species of marine and freshwater fish, including 40 reef-fish species.

Effects of size and temperature were assessed by fitting eqn 5 to metabolic-rate data using non-linear mixed-effects modelling in the R package *lme4* (version 0.999999-0) (Bates *et al.* 2014, Tables S1–S2). During model fitting, thermal regime (E_a) and temperature inactivation (E_i) were treated as having fixed effects. Size (α), temperature activation (E_r), optimum temperature (T_{opt}) and the size- and temperature-corrected rate ($\ln \overline{b_o}(T_c)$) were treated as having both fixed effects and random effects that varied by family ($\Delta\alpha$, ΔE_r , ΔT_{opt} , $\Delta \ln \overline{b_o}(T_c)$). Random effects were assumed to be normally distributed, with means of 0, so the fixed effects α , E_r , T_{opt} and $\ln \overline{b_o}(T_c)$ correspond to family-level averages. Given that thermal regime, $\langle 1/kT \rangle$, was calculated based on the average of the inverse absolute temperature measurements for each family, our approach is mathematically similar to the one described by van de Pol & Wright (2009) for distinguishing within- vs. between-group effects using mixed-effects models.

A parsimonious model that included only the most informative parameters was constructed using maximum likelihood (Zuur *et al.* 2009) (Table S1). This parsimonious model was then refitted using a Bayesian procedure by calling *JAGS* (version 3.3.0) from the R package *R2jags* (version 0.04-01) (Su *et al.* 2014) to determine posterior distributions and associated 95% credible intervals (CIs) for the fitted parameters (R code available at <https://github.com/dbarneche/ELEBarneche>). A key advantage of the Bayesian approach for this analysis was that it allowed us to assess how statistical uncertainties in our estimates for the size and temperature scaling of fish metabolic rates influenced the precision of community-level estimates of size-corrected biomass and energy flux (see hypotheses H4–H5 below). When fitting the models in both *JAGS* and *lme4*, rather than estimate E_r directly, we instead estimated the transformed quantity E'_r , where $E_r = E_i / (1 + \exp(-E'_r))$, to ensure that $E_i > E_r$ in eqn 5 (Tables S2–S3).

Community-level hypotheses

Hypothesis H4: Holding ecosystem net primary productivity constant, size-corrected biomass should decline with increasing temperature.

Community-level flux is equal to the sum of the individual fluxes. Thus, annual respiratory carbon flux for a heterotroph community comprised of J_T individuals in an ecosystem of area A , R_T ($\text{g C m}^{-2} \text{ year}^{-1}$), equals the sum of the time-integrated individual-level respiration rates, $\int_{t=0}^{t=\tau} B_i(t) dt$, over the time interval $t = 0$ day to $t = \tau = 365$ days,

$$R_T = (1/A) \sum_{i=1}^{J_T} \int_{t=0}^{t=\tau} B_i(t) dt = \tau b_o(T_c) M_T \langle M_i^{z-1} \rangle_T \langle e^{E_r(\frac{1}{kT_c} - \frac{1}{kT})} I(T) \rangle_\tau, \quad (6)$$

where $\langle e^{E_r(\frac{1}{kT_c} - \frac{1}{kT})} I(T) \rangle_\tau$ is time-averaged temperature kinetics (Yvon-Durocher *et al.* 2012), which is calculated by integrating temperature variation through time,

$$T(t) = (1/\tau) \int_{t=0}^{t=\tau} e^{E_r(\frac{1}{kT_c} - \frac{1}{kT(t)})} I(T(t)) dt. \quad \text{Community-level size}$$

structure is characterised as $M_T \langle M_i^{z-1} \rangle_T = (1/A) \sum_{i=1}^{J_T} M_i^z$, where M_T is total community biomass per unit area ($= (1/A) \sum_{i=1}^{J_T} M_i$), and $\langle M_i^{z-1} \rangle_T$ is the biomass-weighted average for $M_i^{z-1} = (\sum_{i=1}^{J_T} M_i^z) / (\sum_{i=1}^{J_T} M_i)$ (Allen *et al.* 2005).

We refer to the product $M_T \langle M_i^{z-1} \rangle_T$ as 'size-corrected biomass' because size correction, by $\langle M_i^{z-1} \rangle_T$, accounts for declines in mass-specific metabolic rate, B_i/M_i , with increasing size. This size-related decline is, in turn, predicted by MTE to reflect declines in respiratory capacity (Allen & Gillooly 2009). Consequently, $M_T \langle M_i^{z-1} \rangle_T$ is predicted to be proportional to the total respiratory capacity of the community on a per-unit-area basis (Yvon-Durocher & Allen 2012). Thus, calculation of size-corrected biomass facilitates comparisons of respiratory capacity and energy flux among communities that differ in size structure and standing biomass (Fig. 1).

To derive hypothesis H4 using eqn 6, we note that the reef-fish community garners some fraction, ε_T , of annual NPP, N_T , meaning that $\varepsilon_T N_T = R_T$, and therefore that

$$\ln M_T \langle M_i^{z-1} \rangle_T = \ln[\varepsilon_T / b_o(T_c)] + \ln N_T - \ln \langle e^{E_r(\frac{1}{kT_c} - \frac{1}{kT})} I(T) \rangle_\tau. \quad (7)$$

Holding temperature constant, eqn 7 predicts a proportional increase in total size-corrected biomass with NPP owing to greater food availability, implying a slope of 1 for the second term, $\ln N_T$. Holding NPP constant, it predicts an inverse relationship with time-averaged temperature kinetics owing to increases in per-individual metabolic demands, implying a slope of -1 for the third term. Importantly, these predictions only hold if the fraction of that carbon consumed by the fish community, ε_T , and the size- and temperature-corrected metabolic rate, $b_o(T_c)$, are both independent of thermal regime, and if reefs are relatively closed systems with respect to the production and consumption of reduced carbon. The closed-system assumption, in particular, may not hold true (Hamner *et al.* 1988; Hatcher 1990), but nevertheless provides a point of departure for deriving and testing predictions. Thus, eqn 7 provides a useful benchmark for assessing the extent to which one or more of these assumptions have been violated.

Hypothesis H5: Size-corrected biomass should be lowest at the highest trophic level.

Energy is lost from the system as energy is transferred between trophic levels (Lindeman 1942). Owing to these losses, if reef fishes consumed only autotrophs or other fish occurring on the reef, the fraction of reef NPP garnered by piscivorous fish (ε_{Pi}) would be constrained by energy balance to be lower than that of herbivorous fish (ε_H), meaning that $\varepsilon_{Pi} / \varepsilon_H < 1$. Complications arise, however, because reef fishes consume diverse prey items other than autotrophs and fish, including gastropods and zooplankton. Moreover, higher trophic levels, particularly top predators such as sharks, may receive substantial energy subsidies from outside the system (Trebilco *et al.* 2013).

Despite these complications, we can extend eqn 7 to empirically assess whether energy fluxes of piscivores, R_{Pi} , are lower than those of herbivores, R_H , using data on size-corrected biomass,

$$\ln \frac{R_{P_i}}{R_H} = \ln \frac{M_{P_i} \langle M_i^{\alpha-1} \rangle_{P_i}}{M_H \langle M_i^{\alpha-1} \rangle_H} < 0, \quad (8)$$

where $M_{P_i} \langle M_i^{\alpha-1} \rangle_{P_i}$ ($= (1/A) \sum_{i=1}^{J_{P_i}} M_i^\alpha$) is the size-corrected biomass for J_{P_i} piscivorous individuals in a defined area A , and $M_H \langle M_i^{\alpha-1} \rangle_H$ ($= (1/A) \sum_{i=1}^{J_H} M_i^\alpha$) is the size-corrected biomass for J_H herbivorous individuals in this same area. Importantly, productivity, N_T , and time-averaged temperature kinetics, $\langle e^{E_r(\frac{1}{kT_c} - \frac{1}{kT})} I(T) \rangle_\tau$, both drop out of eqn 8. Consequently, ratios of size-corrected biomass for pairs of trophic groups can be meaningfully compared among communities that differ in size structure, NPP and temperature. These ratios provide a useful, albeit indirect, means of assessing the importance of prey items other than fish. If, for example, the size-corrected biomass of invertivores was higher than that of herbivores in a given community, this would represent direct evidence that the fishes garner more of their energy from invertebrates than from direct consumption of NPP.

Testing hypotheses H4–H5

We evaluated hypotheses H4–H5 using community-level data on reef-fish abundances and body lengths collected from 49 sites (islands, atolls and coastal contiguous reefs), including 14 sites in the South-western Atlantic and its oceanic islands, 1 site in the Caribbean, 2 sites in the Tropical Eastern Atlantic, 1 site in the Tropical Eastern Pacific, 4 sites in the Central Pacific, 2 sites in the South-eastern Pacific and 25 sites in the South Pacific (Table S4). Each species was assigned to one of five trophic groups (herbivores, omnivores, planktivores, invertivores and piscivores) using information in the published literature, online databases and expert judgment (Supplementary Information).

Community-level estimates of size-corrected biomass were inferred from the abundance and body length data by first estimating wet weights of individuals using power-function length-weight conversion formulas compiled from the literature and online databases (Supplementary Information). Fluxes were then estimated by combining size-corrected biomass values with weekly estimates of mean annual sea-surface temperature obtained from the CorTAD database between 1997 and 2007 (Selig *et al.* 2010).

Estimates of ecosystem-level reef NPP are scarce in the literature (Gattuso *et al.* 1998; Naumann *et al.* 2013). Indeed, we are aware of only one study that has estimated it (Odum & Odum 1955). Although many reef studies have reported estimates of net community productivity (NCP; Hatcher 1990), NCP does not represent the total energy available to the heterotrophic community. Rather it is the fixed carbon that remains after heterotrophic consumption (= gross ecosystem photosynthesis – total ecosystem respiration). Consequently, we evaluated Hypothesis H4 for planktivorous fish (i.e. pelagic consumers) using estimates of pelagic NPP (hereafter, N_P , $\text{g C m}^{-2} \text{ year}^{-1}$) derived from SeaWiFS (Behrenfeld & Falkowski 1997). Cautious interpretation is, however, warranted because planktivores may obtain primary production from a larger area owing to oceanic currents (Hamner *et al.* 1988). Data from Abrolhos (South-western Atlantic) were excluded from this analysis because no planktivores were recorded. Uncertainties in the scaling relationships of individual-level

metabolic rates were accounted for by calculating size-corrected biomass, $M_T \langle M_i^{\alpha-1} \rangle_T$, time-averaged temperature kinetics, $\langle e^{E_r(\frac{1}{kT_c} - \frac{1}{kT})} I(T) \rangle_\tau$, and community flux, R_T (in $\text{g C m}^{-2} \text{ yr}^{-1}$), based on the joint posterior distribution for E_r , E_i , T_{opt} , α and $\ln \bar{b}_o(T_c)$ (E_a was not significant, see Results), as determined using Bayesian methods in JAGS.

We evaluated whether the size-corrected biomass of planktivores increased with N_P , and declined with increasing time-average temperature kinetics (hypothesis H4), using standard multiple regression. Two-tailed *t*-tests were used to assess whether the observed slopes differed from expected values. ANCOVA was used to assess whether log ratios of size-corrected biomass (eqn 8) varied in response to temperature and among trophic groups (hypothesis H5). Overall differences in community structure among regions, as indexed by trophic-specific log ratios of size-corrected biomass, were assessed using MANOVA, as is the standard procedure for analysing differences in compositional data (Aitchison 2003). Due to a lack of planktivores, Abrolhos was also excluded from this analysis.

RESULTS AND DISCUSSION

Individual-level hypotheses H1–H3

The parsimonious metabolic-rate model yields estimates for the overall size- and temperature-scaling relationships – representing family-level averages – that closely match MTE Predictions (Tables 1, S1–S3; Figs 2, S1–4). Consistent with hypothesis H1, the overall effect of size, characterized by the scaling exponent α , is statistically indistinguishable from 0.75, implying sub-linear scaling (i.e. $\alpha < 1$), which provides theoretical justification for ‘size-correcting’ biomass at the community level. Consistent with hypothesis H2, the activation energy, E_r , is statistically indistinguishable from the predicted range ~0.6–0.7 eV. Consistent with hypothesis H3, the adaptation parameter E_a is not significant (likelihood ratio test: $\chi^2 = 0.98$; d.f. = 1; $P = 0.323$; Table S1), and is therefore excluded from the parsimonious model (Tables 1, S1–S2). Thus, size- and temperature-corrected rates appear to be largely independent of thermal regime.

Table 1 Average estimates and 95% credible intervals (of Bayesian posterior distributions) for fixed-effects parameters in the parsimonious model (model F2 in Table S1; see Table S3 for estimates of random effects). Fixed-effect parameters include: α , the (family-level) average for the mass dependence of metabolic rate; E_r , the average for the temperature dependence of metabolic rate; $\ln \bar{b}_o(T_c)$, the average for the size-corrected metabolic rate at temperature $T_c = 20^\circ\text{C}$; T_{opt} , the temperature optimum of fish metabolism and E_i , the inactivation energy describing the rate of decline in metabolic rate at temperatures $>T_{opt}$.

Parameter	Estimate	2.5% CI	97.5% CI
Fixed effects			
Size, α	0.760	0.676	0.842
Activation energy, E_r (eV)	0.589	0.430	0.877
Normalisation, $\ln \bar{b}_o(T_c)$ ($\text{g C g}^{-\alpha} \text{ d}^{-1}$)	−5.714	−5.980	−5.274
Temperature optimum, T_{opt} (K)	306.310	301.721	314.562
Inactivation energy, E_i (eV)	2.035	1.248	3.111

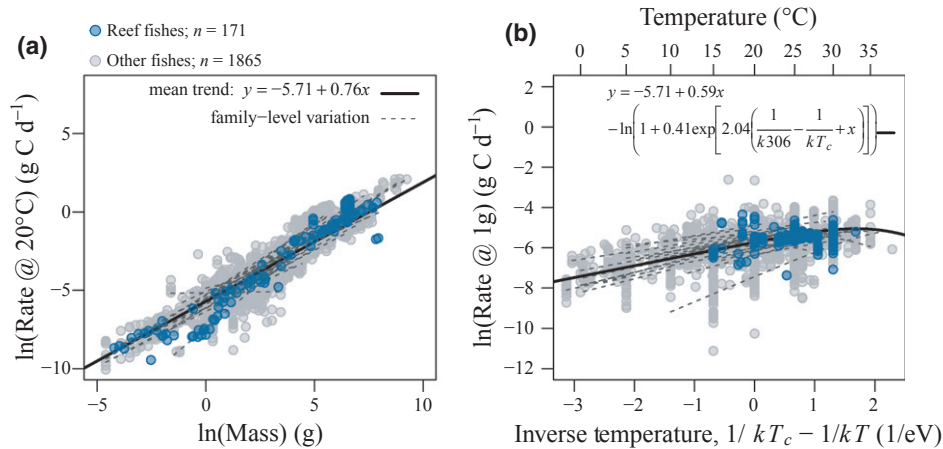


Figure 2 Scaling of routine metabolic rates of fish with respect to (a) body size and (b) temperature. Parameter estimates (listed in Table 1) were obtained using Bayesian methods. The effect of temperature on routine metabolic rate was controlled for in (a) by standardising the temperature measures, T (in K), to $T_c = 293.15$ K (= 20 °C) based on family-level temperature scaling relationships, where k is the Boltzmann constant (8.62×10^{-5} eV K⁻¹). The effect of body mass was controlled for in (b) by standardising measures to 1 gram based on the family-level size scaling relationships. The size-corrected rate at temperature T_c , $\ln \bar{b}_o(T_c) = -5.71$ g C g^{-α} d⁻¹, corresponds to an average across families.

Importantly, however, the temperature inactivation term $I(T)$ (eqn 3) is highly significant (likelihood ratio test: $\chi^2 = 17.04$; d.f. = 6; $P = 0.009$), yielding evidence of a temperature optimum (T_{opt}) for metabolic rates of fish (Fig. S4). By incorporating these parameters into the metabolic-rate model, our analysis expands upon early MTE efforts that described the temperature dependence of biological rates based solely on the Boltzmann relationship (e.g. Gillooly *et al.* 2001; Brown *et al.* 2004; Allen & Gillooly 2009), consistent with other recent MTE work (e.g. Amarasekare & Savage 2012).

Of particular relevance, our estimate for the family-level average for T_{opt} , 33 °C (95% CI: 29–41 °C, Table 1), overlaps with the maximum temperature observed in our sampled tropical reefs (maximum temperature at the sampled sites from CorTAD: 32.55 °C). Analyses of standard metabolic-rate data yield further evidence of a temperature optimum of similar magnitude (Fig. S5). These findings represent independent evidence that at least some marine fish taxa are already experiencing thermal regimes at or near their temperature optima (Gardiner *et al.* 2010), perhaps constraining the capacity of fish communities (and reef ecosystems more generally) to respond to climate change (Rummer *et al.* 2013). Still, it is important to recognise that clear evidence of an optimum is only observed for a subset of the families included in our analysis, which have data that span a wide temperature range (e.g. Centrarchidae, Cyprinidae, Sparidae; Fig. S1). Moreover, the data in our analysis encompass a mixture of short-term acute temperature responses and longer term temperature acclimation, which can occur over multiple generations (Donelson *et al.* 2012). Thus, our findings highlight the need for further investigations on the biochemical mechanisms and timescales of temperature acclimation and adaptation in fish.

After accounting for overall trends using fixed effects, our model reveals substantial family-level variation in size scaling ($\Delta\alpha$), temperature scaling (ΔE_r , ΔT_{opt}) and size- and temperature-corrected rates ($\Delta \ln \bar{b}_o(T_c)$) (Figs. 2, S1). Thus, while our metabolic-rate model supports MTE predictions for fish as a

group, it also quantifies deviations from general trends by incorporating random effects attributable to taxonomy. For example, our estimate of 0.58 for the standard deviation of $\Delta \ln \bar{b}_o(T_c)$ (Table S3) implies that metabolic rate varies, on average, by about 3-fold ($\approx e^{2 \times 0.58}$) among families after accounting for size and temperature. By explicitly accounting for such deviations, modelling approaches such as ours may help to resolve controversies surrounding the generality of metabolic scaling relationships (e.g. Agutter & Wheatley 2004). While the parsimonious model does indicate family-level deviations from α and E_r , 81% of the families had 95% CIs for size-scaling exponents that included the predicted 0.75, and 98% of families had 95% CIs for activation energies that included 0.6–0.7 eV. And, notably, scaling relationships for reef fishes are similar to those of other species (Fig. 2, blue circles).

Community-level hypotheses H4–H5

Propagation of the uncertainties from the individual-level metabolic-rate model to community-level estimates of size-corrected biomass demonstrates that this source of uncertainty introduces error of small magnitude in the estimates of $\ln M_T(M_i^{\alpha-1})_T$ relative to variation among sites (represented by 95% CI bars in Fig. S7). Posterior distributions were therefore averaged to obtain the community-level estimates used in subsequent analyses.

In disagreement with hypothesis H4 (eqn 7), the logarithm of size-corrected biomass for planktivores ($\ln M_P(M_i^{\alpha-1})_P$) is not correlated with time-averaged temperature kinetics ($\ln \langle e^{E_r(\frac{1}{kT_c} - \frac{1}{kT})} I(T) \rangle_t$) or near-pelagic NPP ($\ln N_P$) in a multiple regression analysis ($F = 0.65$, $P = 0.53$). However, after excluding from our analysis six coastal sites in the South-western Atlantic (below 17 °S), all of which are exceptionally turbid (Fig. S8), size-corrected biomass increases significantly ($P < 0.001$) and approximately proportionally with N_P , in agreement with hypothesis H4, as indicated by a log–log slope near 1 from the multiple regression model (1.74, t -test:

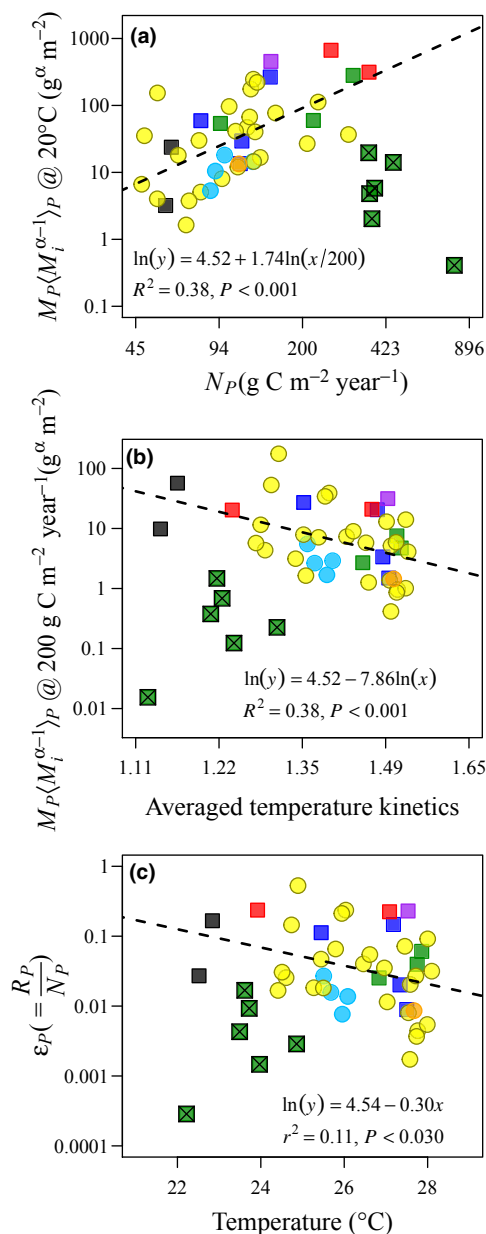


Figure 3 Relationships of size-corrected biomass of planktivores to (a) pelagic net primary production and (b) time-averaged temperature kinetics. (c) Estimated fraction of pelagic net primary productivity respired by planktivores plotted as a function of mean annual temperature. The fitted models and associated statistics depicted in the figure were estimated using multivariate (in a and b) and bivariate (in c) OLS (ordinary least squares) regression, excluding six exceptionally turbid sites (Fig. S8) denoted by 'X' ($n = 42$ sites). The model intercept in panels a and b corresponds to the estimated logarithm of size-corrected biomass for a planktivore community receiving $200 \text{ g C m}^{-2} \text{ year}^{-1}$ at 20°C . Colours are used to denote sites in different regions: South Pacific (yellow), Central Pacific (light blue), South-eastern Pacific (black), Tropical Eastern Pacific (purple), Caribbean (orange), South-western Atlantic (green), South-western Atlantic oceanic islands (blue), Tropical Eastern Atlantic (red). Coral-dominated reefs are depicted as circles and rock-dominated reefs are depicted as squares.

$P = 0.06$; Fig. 3). These findings suggest that planktivore abundances on reefs are constrained by N_P provided that turbidity is not so high that it hampers planktivore feeding

(Johansen & Jones 2013). More generally, they suggest that, despite evidence indicating that local, site-specific hydrodynamics can influence food availability to reef planktivores (Hamner *et al.* 1988), N_P is nevertheless a useful proxy of food availability for reef planktivores at broad spatial scales. Excluding the six turbid sites, the log-log slope of the relationship between size-corrected biomass and time-averaged temperature kinetics is also highly significant in the multiple regression model ($P = 0.004$), but substantially steeper than the predicted -1 (-7.86 , t -test: $P = 0.01$), implying that planktivorous reef fishes garner a progressively smaller fraction of N_P as water temperature increases (Fig. 3c).

Community trophic structure, as indexed by four log ratios of size-corrected biomass (piscivore-to-herbivore, invertivore-to-herbivore, planktivore-to-herbivore and omnivore-to-herbivore, following eqn 8), differs significantly between regions (MANOVA: $P < 0.0001$; Fig. 4), indicating striking differences in resource use among reef-fish communities. For example, size-corrected biomass of planktivores is proportionally higher in the Tropical Eastern Atlantic (63%) than the other regions ($\leq 15\%$; Fig. 4), supporting the idea that plankton can be important energy resources to reef fishes (Hamner *et al.* 1988). Remarkably, these differences in trophic structure are uncorrelated with temperature regime (ANCOVA: $P = 0.5440$; Fig. S7), suggesting primary roles for unmeasured historical factors related to divergent evolutionary histories of distinct fish faunas (Bellwood & Wainwright 2002; Kulbicki *et al.* 2013). In addition, fishing pressure varies considerably among the sites included in our analysis, and can alter community structure (Jackson *et al.* 2001; Sandin *et al.* 2008; Mora *et al.* 2011; Friedlander *et al.* 2013) in diverse ways (Kronen *et al.* 2012). Disentangling human impacts requires careful selection of sites along disturbance gradients (e.g. Sandin *et al.* 2008; McDole *et al.* 2012), and may be informed by the energetic approach adopted here.

Size-corrected biomass also differed among trophic groups, as indicated by significant differences in the averages of the four log ratios (one-way ANOVA: $P < 0.0001$). Consistent with hypothesis H5, the piscivore-to-herbivore log ratio (eqn 8), as well as the planktivore-to-herbivore log ratio, had averages < 0 (two-sided t -tests: both $P < 0.001$), meaning that size-corrected biomass values (and hence energy fluxes) of both groups were less than those of herbivores. However, the mean omnivore-to-herbivore and invertivore-to-herbivore log ratios were not significantly different from 0 (two-sided t -tests: $P = 0.94$ and $P = 0.29$ respectively). *Post hoc* analyses [Tukey HSD (Honestly Significant Difference)] of pair-wise differences among log ratios allow us to construct an average 'stoichiometry' of size-corrected biomass: 4.17 invertivores; 3.09 herbivores; 2.77 omnivores; 1.30 piscivores; 1 planktivore. Thus, in terms of size-corrected biomass, and hence energetics, our results suggest that, on average, invertivores are the most important trophic group in reef-fish communities. These findings indicate that reef-fish communities generally obtain more energy from consumption of invertebrates than from direct consumption of NPP.

Notably, our calculated stoichiometry for size-corrected biomass implies that, on average, energy flux by piscivores is only ~ 2.38 -fold lower than that of herbivores (i.e. $2.38 \approx 3.09/1.30$). This difference is markedly less than would be predicted if

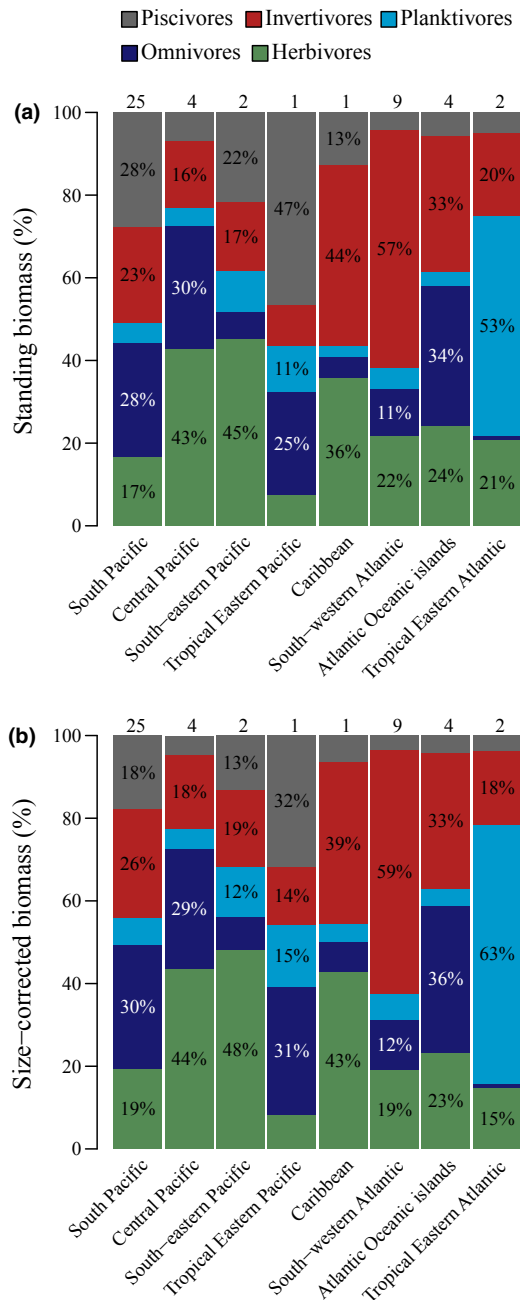


Figure 4 Average percentage allocations of (a) standing biomass and (b) size-corrected biomass among trophic groups for communities in different biogeographic regions. Means of each trophic group were calculated based on log ratios using MANOVA. Numbers on top of the bars indicate the number of sites sampled in each biogeographic region. Only percentages higher than 10% are labelled.

piscivorous reef fish directly or indirectly obtained all of their energy from herbivorous reef fish: assuming a difference of > 2 trophic-position units between herbivores and piscivores (Hussey *et al.* 2014) and a Lindeman (1942) efficiency of ~ 0.10 between adjacent trophic levels, the predicted difference would be > 100 -fold (i.e. $> 0.10^2$). Given that our size-corrected biomass estimates already account for changes in energy use and biomass turnover related to size, body size alone appears insufficient to account for the observation that some pristine reefs

are 'top-heavy', with most biomass in large, apex predators (Sandin *et al.* 2008; Friedlander *et al.* 2013). Rather, our results support the hypothesis that such top-heavy pyramids arise primarily because higher trophic levels receive substantially greater energetic subsidies from sources other than reef fish (Trebilco *et al.* 2013). Contributing factors may include high mobility for large piscivores (Werry *et al.* 2014), which may allow them to garner more energy from areas outside the reef.

More detailed inspection of our size-corrected biomass estimates highlights the importance of size correction for broad-scale comparative analyses. For instance, the percentage standing biomass of piscivores is very high (47%) at the quasi-pristine Isla del Coco (only site in the Tropical Eastern Pacific, Fig. 4a). This pattern reflects the relatively high abundance of large predators, such as the hammerhead shark *Sphyrna lewini* (average biomass of 29.5 kg/sampled individual), which comprises 5% of the standing biomass, but only 2% of the size-corrected biomass. Conversely, the territorial damselfish *Stegastes arcifrons* (average biomass of 0.078 kg/individual) contributes 5% of the standing biomass, but 9% of size-corrected biomass. Consequently, after size correction, relative biomass of piscivores at Isla del Coco becomes significantly smaller (Fig. 4b). These calculations support the assertion that smaller, more abundant fish (e.g. Gobiidae) are often the primary contributors to energy flux in reef-fish communities (Ackerman *et al.* 2004; Depczynski *et al.* 2007).

Total respiratory fluxes of fish communities (eqn 6) increase, on average, ~ 2.3 -fold from 22 to 28°C (Fig. 5). Similar results are obtained if regional effects are explicitly controlled for (Supplementary Information). These respiratory flux estimates are conservative because they exclude contributions of nocturnal fish and of fish < 10 cm (Fig. S6). Still, they exceed estimates of pelagic NPP for 10 of the 49 sites, consistent with observations that the vast majority of primary production on reefs is benthic in origin (Polovina 1984; Naumann *et al.* 2013) and that reef productivity is often substantially higher than the surrounding oceans (Hatcher 1990). The observed increase in total rates of respiration by reef fish with temperature imposes important constraints on the dynamics of reef ecosystems because it implies one or more of the following variables are increasing moving towards warmer reefs: reef fish are garnering a larger fraction of reef NPP, reef NPP is increasing and/or reef fish are receiving greater energy subsidies. Distinguishing among competing mechanisms will require far more extensive data on reef NPP, which is estimated using an approach similar to the one adopted here by first characterising the photosynthetic rates and metabolic demands of autotrophic individuals, and then scaling these fluxes up to entire reef ecosystems (e.g. Odum & Odum 1955; Naumann *et al.* 2013). Thus, the hierarchical statistical approach adopted here, which entails scaling from individuals to ecosystems by explicitly incorporating both idiosyncratic random effects (e.g. taxonomy) and general physiological constraints (e.g. body size, temperature), may prove useful for other groups and applications.

CONCLUSIONS

Our study demonstrates how individual- and community-level data can be combined to identify important broad-scale trends

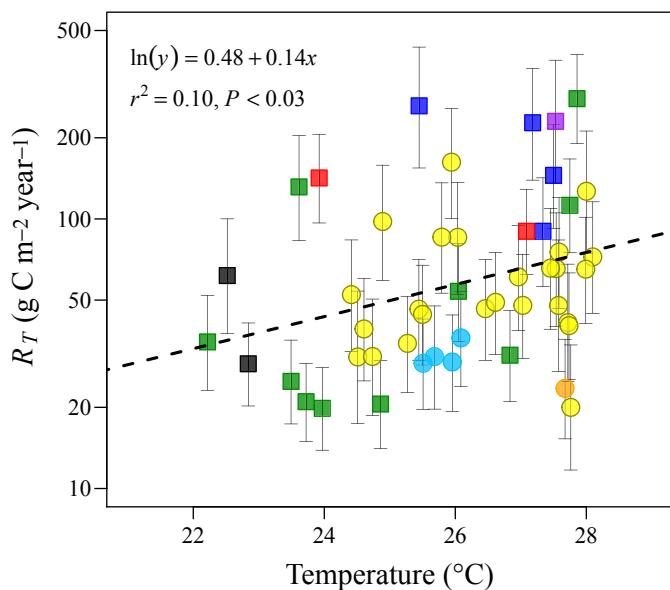


Figure 5 Relationships of mean annual sea surface temperature to total estimated respiratory flux of fish communities. The fitted dashed line and associated statistics were estimated using OLS regression ($n = 49$ sites). The fitted slope implies a ~ 2.3 -fold increase in rates from 22°C to 28°C (i.e. $e^{0.14 \times (28-22)} \approx 2.3$). Colours are used to denote sites in different regions: South Pacific (yellow), Central Pacific (light blue), South-eastern Pacific (black), Tropical Eastern Pacific (purple), Caribbean (orange), South-western Atlantic (green), South-western Atlantic oceanic islands (blue) and Tropical Eastern Atlantic (red). Coral-dominated reefs are depicted as circles, and rock-dominated reefs are depicted as squares. Variation in estimates of community-level flux introduced by statistical uncertainties in the size-temperature scaling of metabolic rate are represented by 95% CI bars in the figure.

in energy flux (Fig. 1). At the individual level, our analyses highlight both the generality of MTE predictions with regard to the size and temperature scaling of metabolic rate, as well as the limitations of these predictions when applied to particular taxonomic groups (Table 1). Our broad-scale comparative approach also yields evidence of a temperature optimum in metabolic rate at $\sim 33^\circ\text{C}$ for many fish taxa (Fig. 2), and thereby reinforces and extends previous work suggesting that at least some tropical reef fishes are already experiencing temperatures near their thermal optima. At the community level, our study highlights the importance and utility of size correction to assess broad-scale gradients in energy flux within and among trophic levels and communities (Fig. 3). Accounting for size in this way reveals striking differences in trophic structure among communities in different oceanic regions (Fig. 4). Finally, by quantifying community-level energy flux, our approach yields important constraints on ecosystem dynamics (Fig. 5).

ACKNOWLEDGEMENTS

We thank V Parravicini for helping with trophic categorisation of reef fishes, EL Rezende for insights into individual-level analyses, all field assistants who helped collecting the data throughout the years and JF Bruno and two anonymous reviewers for insightful feedback on previous versions of this manuscript. This project was supported by Macquarie Univer-

sity (PhD scholarship to D.R.B.), Australian Research Council's Discovery Projects funding scheme (DP0987218 to A.P.A.), CESAB-FRB (Fondation pour la Recherche en Biodiversité), through the GASPARG program, SISBIOTA-Mar (PI: S.R. Floeter CNPq 563276/2010-0 and FAPESC 6308/2011-8), CAPES, Marinha do Brasil, Instituto Laje Viva and the National Geographic Society. The authors declare no conflict of interest.

AUTHORSHIP

D.R.B. and A.P.A. designed the study and hypotheses, developed scripts for data analyses and figures, analysed the data and drafted the manuscript. M.K., S.R.F. and A.M.F. provided reef-fish community data, and J.M. provided turbidity data. All authors contributed substantially to revisions.

REFERENCES

- Ackerman, J.L., Bellwood, D.R. & Brown, J.H. (2004). The contribution of small individuals to density-body size relationships: examination of energetic equivalence in reef fishes. *Oecologia*, 139, 568–571.
- Agutter, P.S. & Wheatley, D.N. (2004). Metabolic scaling: consensus or controversy? *Theor. Biol. Med. Model.*, 1, 13.
- Aitchison, J. (2003). *The Statistical Analysis of Compositional Data*. Blackburn Press, Caldwell, New Jersey, pp. 416.
- Allen, A.P. & Gillooly, J.F. (2009). Towards an integration of ecological stoichiometry and the metabolic theory of ecology to better understand nutrient cycling. *Ecol. Lett.*, 12, 369–384.
- Allen, A.P., Gillooly, J.F. & Brown, J.H. (2005). Linking the global carbon cycle to individual metabolism. *Funct. Ecol.*, 19, 202–213.
- Amarasekare, P. & Savage, V. (2012). A framework for elucidating the temperature dependence of fitness. *Am. Nat.*, 179, 178–191.
- Arias-González, J.E., Delesalle, B., Salvat, B. & Galzin, R. (1997). Trophic functioning of the Tiahura reef sector, Moorea Island, French Polynesia. *Coral Reefs*, 16, 231–246.
- Bates, D., Maechler, M., Bolker, B. & Walker, S. (2014). lme4: Linear mixed-effects models using Eigen and S4. R package version 1.0-6. Available at <http://www.CRAN.R-project.org/package=lme4>.
- Behrenfeld, M.J. & Falkowski, P.G. (1997). Photosynthetic rates derived from satellite-based chlorophyll concentration. *Limnol. Oceanogr.*, 42, 1–20.
- Bellwood, D.R. & Wainwright, P.C. (2002). The history and biogeography of fishes on coral reefs. In: *Coral Reef Fishes: Dynamics and Diversity in a Complex Ecosystem* (ed Sale, P.F.). Academic Press San, Diego, pp. 5–32.
- Bozec, Y.-M., Gascuel, D. & Kulbicki, M. (2004). Trophic model of lagoonal communities in a large open atoll (Uvea, Loyalty islands, New Caledonia). *Aquat. Living Resour.*, 17, 151–162.
- Brown, J.H., Gillooly, J.F., Allen, A.P., Savage, V.M. & West, G.B. (2004). Toward a metabolic theory of ecology. *Ecology*, 85, 1771–1789.
- Clarke, A. & Fraser, K.P.P. (2004). Why does metabolism scale with temperature? *Funct. Ecol.*, 18, 243–251.
- Clarke, A. & Johnston, N.M. (1999). Scaling of metabolic rate with body mass and temperature in teleost fish. *J. Anim. Ecol.*, 68, 893–905.
- Depczynski, M., Fulton, C.J., Marnane, M.J. & Bellwood, D.R. (2007). Life history patterns shape energy allocation among fishes on coral reefs. *Oecologia*, 153, 111–120.
- Donelson, J.M., Munday, P.L., McCormick, M.I. & Pitcher, C.R. (2012). Rapid transgenerational acclimation of a tropical reef fish to climate change. *Nature Clim. Change*, 2, 30–32.
- Friedlander, A.M., Ballesteros, E., Beets, J., Berkenpas, E., Gaymer, C.F., Gorny, M. *et al.* (2013). Effects of isolation and fishing on the

- marine ecosystems of Easter Island and Salas y Gómez. *Chile. Aquat. Conserv.*, 23, 515–531.
- Froese, R. & Pauly, D. (2012). FishBase. World Wide Web electronic publication. Available at <http://www.fishbase.org>. (Version 12/2012). Last accessed 20 January 2014.
- Gardiner, N.M., Munday, P.L. & Nilsson, G.E. (2010). Counter-gradient variation in respiratory performance of coral reef fishes at elevated temperatures. *PLoS ONE*, 5, e13299.
- Gattuso, J.P., Frankignoulle, M. & Wollast, R. (1998). Carbon and carbonate metabolism in coastal aquatic ecosystems. *Annu. Rev. Ecol. Syst.*, 29, 405–434.
- Gillooly, J.F., Brown, J.H., West, G.B., Savage, V.M. & Charnov, E.L. (2001). Effects of size and temperature on metabolic rate. *Science*, 293, 2248–2251.
- Hamner, W.M., Jones, M.S., Carleton, J.H., Hauri, I.R. & Williams, D.M. (1988). Zooplankton, planktivorous fish, and water currents on a windward reef face: Great Barrier Reef, Australia. *Bull. Mar. Sci.*, 42, 459–479.
- Hatcher, B.G. (1990). Coral reef primary productivity. A hierarchy of pattern and process. *Trends Ecol. Evol.*, 5, 149–155.
- Hochachka, P.W. & Somero, G.N. (2002). *Biochemical Adaptation: Mechanism and Process in Physiological Evolution*. Oxford University Press, New York, pp. 480.
- Huey, R.B. & Stevenson, R.D. (1979). Integrating thermal physiology and ecology of ectotherms: a discussion of approaches. *Amer. Zool.*, 19, 357–366.
- Hussey, N.E., MacNeil, M.A., McMeans, B.C., Olin, J.A., Dudley, S.F.J., Cliff, G. *et al.* (2014). Rescaling the trophic structure of marine food webs. *Ecol. Lett.*, 17, 239–250.
- Jackson, J.B., Kirby, M.X., Berger, W.H., Bjorndal, K.A., Botsford, L.W., Bourque, B.J. *et al.* (2001). Historical overfishing and the recent collapse of coastal ecosystems. *Science*, 293, 629–637.
- Johansen, J.L. & Jones, G.P. (2013). Sediment-induced turbidity impairs foraging performance and prey choice of planktivorous coral reef fishes. *Ecol. Appl.*, 23, 1504–1517.
- Kronen, M., Pinca, S., Magron, F., McArdle, B., Vunisea, A., Vigliola, L. *et al.* (2012). Socio-economic and fishery indicators to identify and monitor artisanal finfishing pressure in Pacific Island countries and territories. *Ocean Coast. Manage.*, 55, 63–73.
- Kulbicki, M., Parravicini, V., Bellwood, D.R., Arias-González, E., Chabanet, P., Floeter, S.R. *et al.* (2013). Global biogeography of reef fishes: a hierarchical quantitative delineation of regions. *PLoS ONE*, 8, e81847.
- Lindeman, R.L. (1942). The trophic-dynamic aspect of ecology. *Ecology*, 23, 399–417.
- Lopez-Urrutia, A., San Martin, E., Harris, R.P. & Irigoien, X. (2006). Scaling the metabolic balance of the oceans. *PNAS*, 103, 8739–8744.
- McDole, T., Nulton, J., Barott, K.L., Felts, B., Hand, C., Hatay, M. *et al.* (2012). Assessing Coral Reefs on a Pacific-Wide Scale Using the Microbialization Score. *PLoS ONE*, 7, e43233.
- Mora, C., Aburto-Oropeza, O., Bocos, A.A., Ayotte, P.M., Banks, S., Bauman, A.G. *et al.* (2011). Global human footprint on the linkage between biodiversity and ecosystem functioning in reef fishes. *PLoS Biol.*, 9, e1000606.
- Naumann, M.S., Jantzen, C., Haas, A.F., Iglesias-Prieto, R. & Wild, C. (2013). Benthic primary production budget of a Caribbean reef lagoon (Puerto Morelos, Mexico). *PLoS ONE*, 8, e82923.
- O'Connor, M.I., Piehler, M.F., Leech, D.M., Anton, A. & Bruno, J.F. (2009). Warming and resource availability shift food web structure and metabolism. *PLoS Biol.*, 7, e1000178.
- Odum, H.T. & Odum, E.P. (1955). Trophic structure and productivity of a windward coral reef community on Eniwetok Atoll. *Ecol. Monogr.*, 25, 291–320.
- Parravicini, V., Kulbicki, M., Bellwood, D.R., Friedlander, A.M., Arias-González, J.E., Chabanet, P. *et al.* (2013). Global patterns and predictors of tropical reef fish species richness. *Ecography*, 36, 1254–1262.
- van de Pol, M.V. & Wright, J. (2009). A simple method for distinguishing within- versus between-subject effects using mixed models. *Anim. Behav.*, 77, 753–758.
- Polovina, J. (1984). Model of a coral reef ecosystem. *Coral Reefs*, 3, 1–11.
- Rummer, J.L., Couturier, C.S., Stecyk, J.A.W., Gardiner, N.M., Kinch, J.P., Nilsson, G.E. *et al.* (2013). Life on the edge: thermal optima for aerobic scope of equatorial reef fishes are close to current day temperatures. *Glob. Change Biol.*, 20, 1055–1066.
- Sandin, S.A., Smith, J.E., DeMartini, E.E., Dinsdale, E.A., Donner, S.D., Friedlander, A.M. *et al.* (2008). Baselines and degradation of coral reefs in the northern Line Islands. *PLoS ONE*, 3, e1548.
- Savage, V.M., Gillooly, J.F., Woodruff, W.H., West, G.B., Allen, A.P., Enquist, B.J. *et al.* (2004). The predominance of quarter-power scaling in biology. *Funct. Ecol.*, 18, 257–282.
- Schoolfield, R.M., Sharpe, P.J.H. & Magnuson, C.E. (1981). Non-linear regression of biological temperature-dependent rate models based on absolute reaction-rate theory. *J. Theor. Biol.*, 88, 719–731.
- Selig, E.R., Casey, K.S. & Bruno, J.F. (2010). New insights into global patterns of ocean temperature anomalies: implications for coral reef health and management. *Glob. Ecol. Biogeogr.*, 19, 397–411.
- Su, Y.-S. & Yajima, M. (2014). R2jags: A Package for Running jags from R. R package version 0.04-01.
- Trebilco, R., Baum, J.K., Salomon, A.K. & Dulvy, N.K. (2013). Ecosystem ecology: size-based constraints on the pyramids of life. *Trends Ecol. Evol.*, 28, 423–431.
- Werry, J.M., Planes, S., Berumen, M.L., Lee, K.A., Braun, C.D. & Clua, E. (2014). Reef-fidelity and migration of tiger sharks, *Galeocerdo cuvier*, across the Coral Sea. *PLoS ONE*, 9, e83249.
- Wilson, S.K., Adjeroud, M., Bellwood, D.R., Berumen, M.L., Booth, D., Bozec, Y.M. *et al.* (2010). Crucial knowledge gaps in current understanding of climate change impacts on coral reef fishes. *J. Exp. Biol.*, 213, 894–900.
- Yvon-Durocher, G. & Allen, A.P. (2012). Linking community size structure and ecosystem functioning using metabolic theory. *Philos. Trans. R. Soc. B*, 367, 2998–3007.
- Yvon-Durocher, G., Caffrey, J.M., Cescatti, A., Dossena, M., del Giorgio, P., Gasol, J.M. *et al.* (2012). Reconciling the temperature dependence of respiration across timescales and ecosystem types. *Nature*, 487, 472–476.
- Zuur, A.F., Ieno, E.N., Walker, N.J., Saveliev, A.A. & Smith, G.M. (2009). *Mixed Effects Models and Extensions in Ecology with R*. Springer, New York, p. 574.

SUPPORTING INFORMATION

Additional Supporting Information may be downloaded via the online version of this article at Wiley Online Library (www.ecologyletters.com).

Editor, Boris Worm

Manuscript received 15 January 2014

First decision made 19 February 2014

Manuscript accepted 12 May 2014